



THE UNIVERSITY *of* EDINBURGH

Edinburgh Research Explorer

Cosmological Constraints from Multiple Probes in the Dark Energy Survey

Citation for published version:

(DES Collaboration) 2019, 'Cosmological Constraints from Multiple Probes in the Dark Energy Survey', *Physical Review Letters*, vol. 122, no. 17. <https://doi.org/10.1103/PhysRevLett.122.171301>

Digital Object Identifier (DOI):

[10.1103/PhysRevLett.122.171301](https://doi.org/10.1103/PhysRevLett.122.171301)

Link:

[Link to publication record in Edinburgh Research Explorer](#)

Document Version:

Peer reviewed version

Published In:

Physical Review Letters

General rights

Copyright for the publications made accessible via the Edinburgh Research Explorer is retained by the author(s) and / or other copyright owners and it is a condition of accessing these publications that users recognise and abide by the legal requirements associated with these rights.

Take down policy

The University of Edinburgh has made every reasonable effort to ensure that Edinburgh Research Explorer content complies with UK legislation. If you believe that the public display of this file breaches copyright please contact openaccess@ed.ac.uk providing details, and we will remove access to the work immediately and investigate your claim.



Cosmological Constraints from Multiple Probes in the Dark Energy Survey

T. M. C. Abbott,¹ A. Alarcon,^{2,3} S. Allam,⁴ P. Andersen,^{5,6} F. Andrade-Oliveira,^{7,8} J. Annis,⁴ J. Asorey,⁹ S. Avila,¹⁰ D. Bacon,¹⁰ N. Banik,⁴ B. A. Bassett,^{11,12} E. Baxter,¹³ K. Bechtol,^{14,15} M. R. Becker,¹⁶ G. M. Bernstein,¹³ E. Bertin,^{17,18} J. Blazek,^{19,20} S. L. Bridle,²¹ D. Brooks,²² D. Brout,¹³ D. L. Burke,^{23,24} J. Calcino,⁵ H. Camacho,^{25,8} A. Campos,^{26,7} A. Carnero Rosell,^{27,8} D. Carollo,²⁸ M. Carrasco Kind,^{29,30} J. Carretero,³¹ F. J. Castander,^{2,3} R. Cawthon,¹⁵ P. Challis,³² K. C. Chan,^{2,3} C. Chang,^{33,34} M. Childress,³⁵ M. Crocce,^{2,3} C. E. Cunha,²³ C. B. D'Andrea,¹³ L. N. da Costa,^{8,36} C. Davis,²³ T. M. Davis,⁵ J. De Vicente,²⁷ D. L. DePoy,³⁷ J. DeRose,^{38,23} S. Desai,³⁹ H. T. Diehl,⁴ J. P. Dietrich,^{40,41} S. Dodelson,²⁶ P. Doel,²² A. Drlica-Wagner,^{4,34} T. F. Eifler,^{42,43} J. Elvin-Poole,^{19,44} J. Estrada,⁴ A. E. Evrard,^{45,46} E. Fernandez,³¹ B. Flaugher,⁴ R. J. Foley,⁴⁷ P. Fosalba,^{2,3} J. Frieman,^{4,34} L. Galbany,⁴⁸ J. García-Bellido,⁴⁹ M. Gatti,³¹ E. Gaztanaga,^{2,3} D. W. Gerdes,^{45,46} T. Giannantonio,^{50,51,52} K. Glazebrook,⁵³ D. A. Goldstein,⁵⁴ D. Gruen,^{38,23,24} R. A. Gruendl,^{29,30} J. Gschwend,^{8,36} G. Gutierrez,⁴ W. G. Hartley,^{22,55} S. R. Hinton,⁵ D. L. Hollowood,⁴⁷ K. Honscheid,^{19,44} J. K. Hoormann,⁵ B. Hoyle,^{56,52} D. Huterer,⁴⁶ B. Jain,¹³ D. J. James,⁵⁷ M. Jarvis,¹³ T. Jeltema,⁴⁷ E. Kasai,^{58,12} S. Kent,^{4,34} R. Kessler,^{33,34} A. G. Kim,⁵⁹ N. Kokron,^{38,23} E. Krause,⁴² R. Kron,^{4,34} K. Kuehn,⁶⁰ N. Kuropatkin,⁴ O. Lahav,²² J. Lasker,^{33,34} P. Lemos,^{22,50,51} G. F. Lewis,⁶¹ T. S. Li,^{4,34} C. Lidman,⁶² M. Lima,^{25,8} H. Lin,⁴ E. Macaulay,¹⁰ N. MacCrann,^{19,44} M. A. G. Maia,^{8,36} M. March,¹³ J. Marriner,⁴ J. L. Marshall,³⁷ P. Martini,^{19,63} R. G. McMahon,^{50,51} P. Melchior,⁶⁴ F. Menanteau,^{29,30} R. Miquel,^{65,31} J. J. Mohr,^{40,41,56} E. Morganson,³⁰ J. Muir,²³ A. Möller,^{66,62} E. Neilsen,⁴ R. C. Nichol,¹⁰ B. Nord,⁴ R. L. C. Ogando,^{8,36} A. Palmese,⁴ Y.-C. Pan,^{67,68} H. V. Peiris,²² W. J. Percival,^{69,70} A. A. Plazas,⁶⁴ A. Porredon,^{2,3} J. Prat,³¹ A. K. Romer,⁷¹ A. Roodman,^{23,24} R. Rosenfeld,^{72,8} A. J. Ross,¹⁹ E. S. Rykoff,^{23,24} S. Samuroff,²⁶ C. Sánchez,¹³ E. Sanchez,²⁷ V. Scarpine,⁴ R. Schindler,²⁴ M. Schubnell,⁴⁶ D. Scolnic,³⁴ L. F. Secco,¹³ S. Serrano,^{2,3} I. Sevilla-Noarbe,²⁷ R. Sharp,⁶² E. Sheldon,⁷³ M. Smith,³⁵ M. Soares-Santos,⁷⁴ F. Sobreira,^{75,8} N. E. Sommer,^{66,62} E. Swann,¹⁰ M. E. C. Swanson,³⁰ G. Tarle,⁴⁶ D. Thomas,¹⁰ R. C. Thomas,⁵⁹ M. A. Troxel,⁷⁶ B. E. Tucker,^{66,62} S. A. Uddin,⁷⁷ P. Vielzeuf,³¹ A. R. Walker,¹ M. Wang,⁴ N. Weaverdyck,⁴⁶ R. H. Wechsler,^{38,23,24} J. Weller,^{40,56,52} B. Yanny,⁴ B. Zhang,^{66,62} Y. Zhang,⁴ and J. Zuntz⁷⁸

(DES Collaboration)

¹*Cerro Tololo Inter-American Observatory, National Optical Astronomy Observatory, Casilla 603, La Serena, Chile*

²*Institut d'Estudis Espacials de Catalunya (IEEC), 08034 Barcelona, Spain*

³*Institute of Space Sciences (ICE, CSIC), Campus UAB, Carrer de Can Magrans, s/n, 08193 Barcelona, Spain*

⁴*Fermi National Accelerator Laboratory, P. O. Box 500, Batavia, IL 60510, USA*

⁵*School of Mathematics and Physics, University of Queensland, Brisbane, QLD 4072, Australia*

⁶*University of Copenhagen, Dark Cosmology Centre, Juliane Maries Vej 30, 2100 Copenhagen O*

⁷*Instituto de Física Teórica, Universidade Estadual Paulista, São Paulo, Brazil*

⁸*Laboratório Interinstitucional de e-Astronomia - LInEA, Rua Gal. José Cristino 77, Rio de Janeiro, RJ - 20921-400, Brazil*

⁹*Korea Astronomy and Space Science Institute, Yuseong-gu, Daejeon, 305-348, Korea*

¹⁰*Institute of Cosmology and Gravitation, University of Portsmouth, Portsmouth, PO1 3FX, UK*

¹¹*African Institute for Mathematical Sciences, 6 Melrose Road, Muizenberg, 7945, South Africa*

¹²*South African Astronomical Observatory, P.O.Box 9, Observatory 7935, South Africa*

¹³*Department of Physics and Astronomy, University of Pennsylvania, Philadelphia, PA 19104, USA*

¹⁴*LSSST, 933 North Cherry Avenue, Tucson, AZ 85721, USA*

¹⁵*Physics Department, 2320 Chamberlin Hall, University of Wisconsin-Madison, 1150 University Avenue Madison, WI 53706-1390*

¹⁶*Argonne National Laboratory, 9700 South Cass Avenue, Lemont, IL 60439, USA*

¹⁷*CNRS, UMR 7095, Institut d'Astrophysique de Paris, F-75014, Paris, France*

¹⁸*Sorbonne Universités, UPMC Univ Paris 06, UMR 7095, Institut d'Astrophysique de Paris, F-75014, Paris, France*

¹⁹*Center for Cosmology and Astro-Particle Physics, The Ohio State University, Columbus, OH 43210, USA*

²⁰*Institute of Physics, Laboratory of Astrophysics, École Polytechnique Fédérale de Lausanne (EPFL), Observatoire de Sauverny, 1290 Versoix, Switzerland*

²¹*Jodrell Bank Center for Astrophysics, School of Physics and Astronomy, University of Manchester, Oxford Road, Manchester, M13 9PL, UK*

²²*Department of Physics & Astronomy, University College London, Gower Street, London, WC1E 6BT, UK*

²³*Kavli Institute for Particle Astrophysics & Cosmology, P. O. Box 2450, Stanford University, Stanford, CA 94305, USA*

²⁴*SLAC National Accelerator Laboratory, Menlo Park, CA 94025, USA*

²⁵*Departamento de Física Matemática, Instituto de Física, Universidade de São Paulo, CP 66318, São Paulo, SP, 05314-970, Brazil*

²⁶*Department of Physics, Carnegie Mellon University, Pittsburgh, Pennsylvania 15312, USA*

²⁷*Centro de Investigaciones Energéticas, Medioambientales y Tecnológicas (CIEMAT), Madrid, Spain*

- ²⁸INAF, Astrophysical Observatory of Turin, I-10025 Pino Torinese, Italy
- ²⁹Department of Astronomy, University of Illinois at Urbana-Champaign, 1002 W. Green Street, Urbana, IL 61801, USA
- ³⁰National Center for Supercomputing Applications, 1205 West Clark St., Urbana, IL 61801, USA
- ³¹Institut de Física d'Altes Energies (IFAE), The Barcelona Institute of Science and Technology, Campus UAB, 08193 Bellaterra (Barcelona) Spain
- ³²Harvard-Smithsonian Center for Astrophysics, 60 Garden St., Cambridge, MA 02138, USA
- ³³Department of Astronomy and Astrophysics, University of Chicago, Chicago, IL 60637, USA
- ³⁴Kavli Institute for Cosmological Physics, University of Chicago, Chicago, IL 60637, USA
- ³⁵School of Physics and Astronomy, University of Southampton, Southampton, SO17 1BJ, UK
- ³⁶Observatório Nacional, Rua Gal. José Cristino 77, Rio de Janeiro, RJ - 20921-400, Brazil
- ³⁷George P. and Cynthia Woods Mitchell Institute for Fundamental Physics and Astronomy, and Department of Physics and Astronomy, Texas A&M University, College Station, TX 77843, USA
- ³⁸Department of Physics, Stanford University, 382 Via Pueblo Mall, Stanford, CA 94305, USA
- ³⁹Department of Physics, IIT Hyderabad, Kandi, Telangana 502285, India
- ⁴⁰Excellence Cluster Universe, Boltzmannstr. 2, 85748 Garching, Germany
- ⁴¹Faculty of Physics, Ludwig-Maximilians-Universität, Scheinerstr. 1, 81679 Munich, Germany
- ⁴²Department of Astronomy/Steward Observatory, 933 North Cherry Avenue, Tucson, AZ 85721-0065, USA
- ⁴³Jet Propulsion Laboratory, California Institute of Technology, 4800 Oak Grove Dr., Pasadena, CA 91109, USA
- ⁴⁴Department of Physics, The Ohio State University, Columbus, OH 43210, USA
- ⁴⁵Department of Astronomy, University of Michigan, Ann Arbor, MI 48109, USA
- ⁴⁶Department of Physics, University of Michigan, Ann Arbor, MI 48109, USA
- ⁴⁷Santa Cruz Institute for Particle Physics, Santa Cruz, CA 95064, USA
- ⁴⁸PITT PACC, Department of Physics and Astronomy, University of Pittsburgh, Pittsburgh, PA 15260, USA
- ⁴⁹Instituto de Física Teórica UAM/CSIC, Universidad Autónoma de Madrid, 28049 Madrid, Spain
- ⁵⁰Institute of Astronomy, University of Cambridge, Madingley Road, Cambridge CB3 0HA, UK
- ⁵¹Kavli Institute for Cosmology, University of Cambridge, Madingley Road, Cambridge CB3 0HA, UK
- ⁵²Universitäts-Sternwarte, Fakultät für Physik, Ludwig-Maximilians Universität München, Scheinerstr. 1, 81679 München, Germany
- ⁵³Centre for Astrophysics & Supercomputing, Swinburne University of Technology, Victoria 3122, Australia
- ⁵⁴California Institute of Technology, 1200 East California Blvd, MC 249-17, Pasadena, CA 91125, USA
- ⁵⁵Department of Physics, ETH Zurich, Wolfgang-Pauli-Strasse 16, CH-8093 Zurich, Switzerland
- ⁵⁶Max Planck Institute for Extraterrestrial Physics, Giessenbachstrasse, 85748 Garching, Germany
- ⁵⁷Harvard-Smithsonian Center for Astrophysics, Cambridge, MA 02138, USA
- ⁵⁸Department of Physics, University of Namibia, 340 Mandume Ndemufayo Avenue, Pionierspark, Windhoek, Namibia
- ⁵⁹Lawrence Berkeley National Laboratory, 1 Cyclotron Road, Berkeley, CA 94720, USA
- ⁶⁰Australian Astronomical Optics, Macquarie University, North Ryde, NSW 2113, Australia
- ⁶¹Sydney Institute for Astronomy, School of Physics, A28, The University of Sydney, NSW 2006, Australia
- ⁶²The Research School of Astronomy and Astrophysics, Australian National University, ACT 2601, Australia
- ⁶³Department of Astronomy, The Ohio State University, Columbus, OH 43210, USA
- ⁶⁴Department of Astrophysical Sciences, Princeton University, Peyton Hall, Princeton, NJ 08544, USA
- ⁶⁵Institució Catalana de Recerca i Estudis Avançats, E-08010 Barcelona, Spain
- ⁶⁶ARC Centre of Excellence for All-sky Astrophysics (CAASTRO)
- ⁶⁷Division of Theoretical Astronomy, National Astronomical Observatory of Japan, 2-21-1 Osawa, Mitaka, Tokyo 181-8588, Japan
- ⁶⁸Institute of Astronomy and Astrophysics, Academia Sinica, Taipei 10617, Taiwan
- ⁶⁹Department of Physics and Astronomy, University of Waterloo, 200 University Ave W, Waterloo, ON N2L 3G1, Canada
- ⁷⁰Perimeter Institute for Theoretical Physics, 31 Caroline St. North, Waterloo, ON N2L 2Y5, Canada
- ⁷¹Department of Physics and Astronomy, Pevensey Building, University of Sussex, Brighton, BN1 9QH, UK
- ⁷²ICTP South American Institute for Fundamental Research
Instituto de Física Teórica, Universidade Estadual Paulista, São Paulo, Brazil
- ⁷³Brookhaven National Laboratory, Bldg 510, Upton, NY 11973, USA
- ⁷⁴Brandeis University, Physics Department, 415 South Street, Waltham MA 02453
- ⁷⁵Instituto de Física Gleb Wataghin, Universidade Estadual de Campinas, 13083-859, Campinas, SP, Brazil
- ⁷⁶Department of Physics, Duke University, Durham, NC 27708, USA
- ⁷⁷Observatories of the Carnegie Institution for Science, 813 Santa Barbara St., Pasadena, CA 91101, USA
- ⁷⁸Institute for Astronomy, University of Edinburgh, Edinburgh EH9 3HJ, UK

(Dated: May 7, 2019)

The combination of multiple observational probes has long been advocated as a powerful technique to constrain cosmological parameters, in particular dark energy. The Dark Energy Survey has measured 207 spectroscopically-confirmed Type Ia supernova lightcurves; the baryon acoustic oscillation feature; weak gravitational lensing; and galaxy clustering. Here we present combined results from these probes, deriving constraints on the equation of state, w , of dark energy and its energy density in the Universe. Independently of other experiments, such as those that measure the cosmic microwave background, the probes from this single photometric

survey rule out a Universe with no dark energy, finding $w = -0.80_{-0.11}^{+0.09}$. The geometry is shown to be consistent with a spatially flat Universe, and we obtain a constraint on the baryon density of $\Omega_b = 0.069_{-0.012}^{+0.009}$ that is independent of early Universe measurements. These results demonstrate the potential power of large multi-probe photometric surveys and pave the way for order of magnitude advances in our constraints on properties of dark energy and cosmology over the next decade.

Keywords: dark energy; dark matter; cosmology: observations; cosmological parameters

INTRODUCTION

The discovery of the accelerating Universe [1, 2] revolutionized 20th century cosmology by indicating the presence of a qualitatively new component in the Universe that dominates the expansion in the last several billion years. The nature of dark energy — the component that causes the accelerated expansion — is unknown, and understanding its properties and origin is one of the principal challenges in modern physics. Current measurements are consistent with an interpretation of dark energy as a cosmological constant in General Relativity. Any deviation from this interpretation in space or time would constitute a landmark discovery in fundamental physics [3].

Dark energy leaves imprints on cosmological observations, typically split into two regimes — 1) it modifies the geometry of the Universe, increasing distances and volumes in the Universe over time via the accelerated expansion, and 2) it suppresses the growth of cosmic structure. However, these effects can be mimicked by the variation of other cosmological parameters, including the dark matter density and curvature, or other physical models and systematics that are degenerate within a single probe. Consequently, measuring dark energy properties requires a combination of cosmological probes that are sensitive to both classes of effects to break these parameter and model degeneracies [4–6].

Historically, the most powerful cosmic probe has been the cosmic microwave background (CMB) [7–9], relic radiation from the surface of last scattering only 400,000 years after the Big Bang. Low-redshift probes measure the Universe over the last several billion years, when dark energy dominates the expansion. Comparing or combining constraints between the CMB and lower redshift measurements requires us to extrapolate predictions to the present-day Universe starting from initial conditions over 13 billion years ago. This is a powerful test of our models, but it requires precise, independent constraints from low-redshift experiments. Low-redshift probes include Type Ia supernova (SNe Ia) measurements, which treat the SNe Ia as standardizable candles and employ redshift and flux measurements to probe the redshift-luminosity distance relation [10]; baryon acoustic oscillations (BAO), which use a ‘standard ruler’ scale in the cosmic density field, imprinted by sound waves at recombination, to probe several redshift-distance combinations [11, 12]; galaxy clustering, which measures the density field up to some bias between galaxy density and the underlying dark matter density, and redshift-space distortions (RSD) in the clustering [13]; the counts of galaxy clusters, representing the most extreme density peaks in the Universe [14]; strong gravitational lensing

[15]; and weak gravitational lensing, which probes changes in the gravitational potential along the line of sight using coherent distortions in observed properties of galaxies or the CMB, e.g. to measure the dark and baryonic matter distribution [16].

We report here the first results from the Dark Energy Survey (DES) combining precision probes of both geometry and growth of structure that include BAO, SNe Ia, and weak lensing and galaxy clustering from a single experiment. DES has previously shown separate cosmological constraints using weak lensing and galaxy clustering [17], BAO [18], and SNe Ia [19]. We now combine these probes and begin to fully realize the power of this multi-probe experiment to produce independent measurements of the properties of dark energy.

The work presented here demonstrates our ability to extract and combine diverse cosmological observables from wide-field surveys of the evolved Universe. Previous dark energy constraints have relied on combining the likelihoods of many separate and independent experiments to produce precise constraints on cosmological models including dark energy. For this traditional approach each experiment has performed an independent analysis to validate measurements and has separate calibration methodologies and requirements, thus ensuring that many potential systematics are uncorrelated between probes. The DES analysis presented here, however, uses a common set of both calibration methodologies and systematics modeling and marginalization across probes, which enables a consistently validated analysis. Perhaps most importantly, this common framework allows us to standardize requirements like blinding across these probes, which is essential to minimize the impact of experimenter bias [20]. This approach provides a very robust, precise cross-check of traditional multi-probe analyses, which currently provide tighter overall constraints.

The fundamental interest in understanding the nature of dark energy has spurred the development of multiple large photometric surveys that image the sky, capable of independently combining multiple cosmic probes. The current generation of surveys includes the Hyper-Suprime Cam survey (HSC) [21], the Kilo-Degree Survey (KiDS) [22], and the focus of this work, DES [23]. The next generation of these surveys will include the Large Synoptic Survey Telescope (LSST) [24], a ground-based telescope that will observe the entire southern hemisphere with very high cadence, and space telescopes Euclid [25] and the Wide-Field InfraRed Survey Telescope (WFIRST) [26]. In parallel with imaging surveys, the distribution of galaxies measured by spectroscopic surveys (i.e., BOSS [27], eBOSS [28], and the planned 4MOST [29], DESI [30], and PFS [31] surveys) provides powerful con-

straints on the distance-redshift relation via BAO measurements and the growth of structure via redshift space distortions. The union of these results over the following several years, and into the next decades, will ensure that we are able to take advantage of the benefits of multiple independent, self-consistent, and blinded multi-probe analyses like we present here for DES.

COSMIC PROBES

The Dark Energy Survey

DES cosmic probes span a wide range of redshifts up to $z \approx 1.3$, and include weak gravitational lensing and galaxy clustering due to large-scale structure [17], SNe Ia [19], and BAO [18]. Each probe constrains dark energy independently and their combination is more powerful. These probes utilize a subset of data from DES taken during its first three observing seasons (Aug. 2013 to Feb. 2016). Spectroscopically confirmed SNe Ia are identified from images in all three seasons (DES Y3) in 27 deg^2 of repeated deep-field observations, while weak lensing and large-scale structure information is derived from images taken only in the first season (DES Y1), ending Feb. 2014 and covering 1321 deg^2 of the southern sky in *grizY* filters. DES uses the 570-megapixel Dark Energy Camera (DECam [32]) at the Cerro Tololo Inter-American Observatory (CTIO) 4m Blanco telescope in Chile. By the end of DES observations in January 2019, we anticipate an order of magnitude increase in the number of useable SNe, while the area of sky used for the other probes will increase by a factor of three to 5000 deg^2 . Analysis of the later years of survey data is ongoing.

Data is processed through the DES Data Management system [33–36]. This system detrends and calibrates the raw images, creates coadded images from individual exposures, and detects and catalogs astrophysical objects. This catalog is further cleaned and calibrated to create a high-quality (‘Gold’) object catalog [37] from which weak lensing and large-scale structure measurements are made. The deep fields are also processed through a separate difference imaging pipeline to identify transients [38, 39]. The photometric and astrometric calibrations [37] are common to all cosmology probes discussed below.

Weak Gravitational Lensing and Large-Scale Structure

For weak gravitational lensing measurements, we use the measured shapes and positions of 26 million galaxies in the redshift range $0.2 < z < 1.3$, split into four redshift bins. The galaxy shapes are measured via the METACALIBRATION method [40, 41] using *riz*-band exposures [42]. Photometric redshifts for the objects are determined from a modified version of the BPZ method [43], described and calibrated in Ref. [44].

For measurements of the angular galaxy clustering, we utilize the positions of a sample of luminous red galaxies that have precise photometric redshifts selected with the REDMAGIC algorithm [45]. This results in a sample of 650,000 galaxies over the redshift range $0.15 < z < 0.9$, split into five narrow redshift bins. Residual correlations of number density with survey conditions in the REDMAGIC sample are calibrated in Ref. [46]. The precise redshifts of REDMAGIC galaxies allow us to infer information about the more poorly constrained photo- z bias uncertainty in the weak lensing catalog. The photo- z calibration methodology is consistent between the weak lensing and REDMAGIC samples [44, 47–49].

We use measurements from each of these galaxy samples to construct a set of three two-point correlation function observables we label ‘ $3 \times 2pt$ ’. These include the galaxy shear auto-correlation (cosmic shear), the galaxy position-shear cross-correlation (galaxy-galaxy lensing), and the galaxy position auto-correlation (galaxy clustering). The analysis was described in a series of papers that include the covariance and analysis framework [50, 51], the measurements and validation [46, 52–54], and the cosmological results [17]. We utilize the ‘ $3 \times 2pt$ ’ likelihood pipeline from this set of papers as implemented in COSMOSIS [55]. This combination of probes produces a tight constraint on the amplitude of matter clustering in the Universe and on the properties of dark energy over the last six billion years.

Type Ia Supernovae

The DES-SN sample is comprised of 207 spectroscopically confirmed SNe Ia in the redshift range $0.07 < z < 0.85$. The sample-building and analysis pipelines are discussed in a series of papers that detail the SN Ia search and discovery [36, 38, 39]; spectroscopic follow-up [56]; photometry [57]; calibration [58, 59]; simulations [60]; and technique of accounting for selection bias [61, 62]. The analysis methodology and systematic uncertainties are presented in Ref. [63]. These results are used to constrain cosmology [19] and the Hubble constant [64]. In Refs. [19, 63, 64] the DES-SN sample is combined with a ‘Low- z ’ ($z < 0.1$) sample, which includes SNe from the Harvard-Smithsonian Center for Astrophysics surveys [65, 66] and the Carnegie Supernova Project [67]. Selection effects and calibration of these low-redshift samples is discussed in [10]. Here we fit for DES-SN alone, and only include the Low- z sample for comparison to Ref. [19]. We compute the SNe likelihood using the SNe module [10] implemented in COSMOSIS, which is able to reproduce the results in [19].

Baryon Acoustic Oscillations

A sample of 1.3 million galaxies from the DES Y1 ‘Gold’ catalog in the redshift range $0.6 < z < 1.0$ was used to measure the BAO scale in the distribution of galaxies. De-

tails of the galaxy sample selection are in Ref. [68]. Calibrations of the galaxy selection function are consistently derived for the BAO and ‘3×2pt’ samples. This BAO measurement was presented in Ref. [18] and provides a likelihood for the ratio between the angular diameter distance to redshift 0.81, $D_A(z = 0.81)$, and the sound horizon at the drag epoch, r_d . This analysis used 1800 simulations [69] and three methods to compute the galaxy clustering [70–72]. The BAO likelihood is implemented in COSMOSIS. The galaxy samples used in the ‘3×2pt’ angular clustering measurements and in the BAO analysis share a common footprint in the sky and overlap significantly in volume over the redshift range $0.6 < z < 0.9$, which will produce some non-zero correlation between the two measurements. However, the intersection of the galaxy populations is only about 14% of the total BAO galaxy sample and we detect no significant BAO constraint when using the ‘3x2pt’ galaxy clustering measurements. We thus ignore this negligible correlation when combining the two probes.

External Data for Comparison

We use external constraints that combine state-of-the-art CMB, SNe Ia, and spectroscopic BAO measurements to compare our results against. For the CMB data, we utilize full-sky temperature (T) and polarization (E - and B -mode) measurements from the Planck survey, combining TT ($\ell \in [2, 2508]$), and EE , BB and TE ($\ell \in [2, 29]$) (commonly referred to as ‘TT+LowP’) [73] with weak lensing measurements derived from the temperature data [74]. We use the Planck likelihood from Ref. [75].

For external SNe Ia measurements, we use the Pantheon compilation [10]. Pantheon combines SNe Ia samples from Pan-STARRS1, SDSS, SNLS, various low- z data sets, and HST. The Pantheon data set is based on the Pan-STARRS1 Supercal algorithm [76] that establishes a global calibration for the 13 different SNe Ia samples, with a total of 1048 SNe in $0.01 < z < 2.26$.

Finally, external spectroscopic BAO measurements are taken from BOSS DR12 [13], the 6dF Galaxy Survey [77], and the SDSS Main Galaxy Sample [78]. These measurements of the BAO scale span a redshift range of $0.1 < z < 0.6$.

CONSTRAINTS ON DARK ENERGY

We present here a dark energy analysis that combines for the first time the DES probes described above. DES is able to strongly constrain dark energy models without the CMB by probing over a wide redshift range ($z \lesssim 1$) the growth of structure and distance-redshift relation, which are both sensitive to the presence of dark energy. The dark energy equation of state w relates the pressure (P) to the energy density (ρ) of the dark energy fluid: $w = P/\rho$, where $w = -1$ is equivalent to a cosmological constant Λ in the field equations. We probe

TABLE I. Cosmological parameter constraints in the Λ CDM and w CDM models using only DES data. We report the 1D peak of the posterior and asymmetric 68% confidence limits. The marginalized parameters with informative priors (and prior ranges) are: the primordial perturbation amplitude $10^9 A_s \in [0.5, 10.0]$, the Hubble constant $H_0 \in [55, 90]$ km s $^{-1}$ Mpc $^{-1}$, the spectral index $n_s \in [0.87, 1.07]$, and the neutrino mass density $\Omega_\nu h^2 \in [0.0006, 0.01]$.

Parameter	Λ CDM	w CDM	w CDM (Ext)	Flat Prior
Ω_m	$0.299^{+0.024}_{-0.020}$	$0.300^{+0.023}_{-0.021}$	$0.303^{+0.007}_{-0.009}$	[0.1, 0.9]
Ω_b	$0.069^{+0.009}_{-0.012}$	$0.064^{+0.013}_{-0.009}$	$0.048^{+0.001}_{-0.001}$	[0.03, 0.12]
Ω_k	$0.252^{+0.095}_{-0.14}$	0	0	[-0.1, 0.5]
Ω_Λ	$0.47^{+0.14}_{-0.12}$	$0.700^{+0.021}_{-0.023}$	$0.697^{+0.009}_{-0.007}$	Derived
w	-1	$-0.80^{+0.09}_{-0.11}$	$-1.02^{+0.03}_{-0.04}$	[-2, -0.33]
S_8	$0.801^{+0.028}_{-0.026}$	$0.786^{+0.029}_{-0.019}$	$0.814^{+0.016}_{-0.011}$	Derived

the nature of dark energy in two ways: 1) we constrain the dark energy density relative to the critical density today, Ω_Λ , assuming that dark energy takes the form of a cosmological constant and allowing non-zero curvature (the Λ CDM model), and 2) we measure w as a free parameter (the w CDM model) with fixed curvature ($\Omega_k = 0$). The total energy density of the Universe today is composed of the sum of fractional components $1 = \Omega_k + \Omega_m + \Omega_\Lambda$, where the components are: curvature (Ω_k), the total matter (Ω_m), and dark energy (Ω_Λ). The radiation density is assumed to be negligible over the redshift ranges probed by DES.

In both Λ CDM and w CDM models, we explore the ability of DES to constrain these properties of dark energy and compare this to the state-of-the-art constraints combining measurements from many external surveys. We follow the analysis methods and model definitions from Ref. [17], which includes varying the neutrino mass density in all models. External data are re-analyzed to make direct comparisons meaningful, including matching parameter choices and priors to the DES analysis. The cosmological parameters and their priors are slightly changed from Ref. [17] and listed in Table I. Non-cosmological parameters and their priors are identical to Table 1 of Ref. [17], with the absolute magnitude $-19.5 < \mathcal{M} < -18.9$ for SNe. Cosmological parameters and the intrinsic alignment model (for ‘3×2pt’) are shared between probes. The joint posterior is the product of the individual posteriors of the three probes, which are assumed to be sufficiently independent at this precision, as motivated in the previous section.

Figure 1 shows our constraints on Ω_Λ in the Λ CDM model, where $w = -1$. We combine our ‘3×2pt’, SNe Ia (without the external Low- z sample), and photometric BAO measurements to constrain Ω_Λ and Ω_m . This is compared to the constraint from the external data sets. The DES best-fit χ^2 is 576 with 498 degrees of freedom (dof) [79]. Using DES data we are able to independently confirm the existence of a dark energy

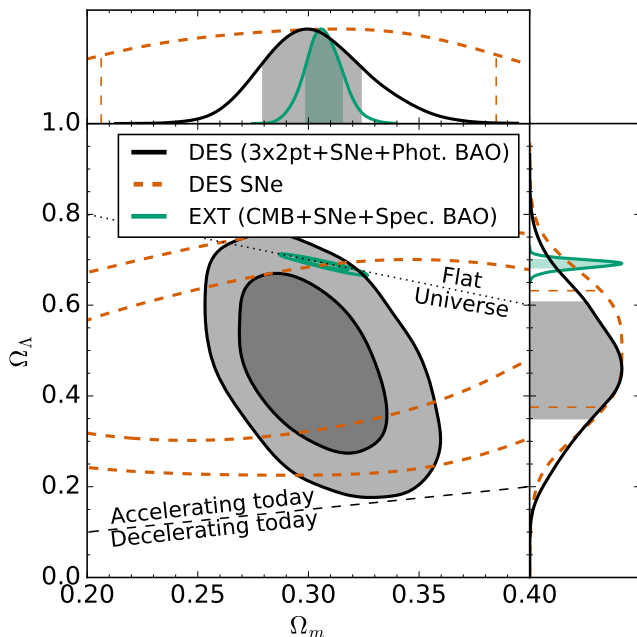


FIG. 1. Constraints on the present-day dark energy density Ω_Λ and matter density Ω_m , relative to the critical density, in an Λ CDM model with marginalized curvature and neutrino mass density. We compare the constraint from DES data alone (black contours), including information from weak gravitational lensing, large-scale structure, SNe Ia, and photometric BAO, to the best available external data (green contours), combining information from the CMB, SNe Ia, and spectroscopic BAO. We identify the flat model ($\Omega_k = 0$) with a dotted line and distinguish accelerating and decelerating universes with a dashed line. Contours represent the 68% and 95% confidence limits (CL).

component in the Universe ($\Omega_\Lambda > 0$) at $\sim 4\sigma$ significance. This is the first time a photometric survey has independently made a significant constraint on the energy density of both dark energy and dark matter without assuming a flat model based on early Universe constraints. It represents an important milestone for future analyses from DES and surveys like Euclid, LSST, and WFIRST.

In Fig. 2, we show the constraint on w and Ω_m , assuming the w CDM model. We show the same comparison with external data as in Fig. 1, but also include a case where we supplement DES-discovered SNe Ia with the Low- z SNe sample to anchor the SNe redshift-distance relation at low redshift following Ref. [19]. This low-redshift SNe anchor contributes significantly to both the DES+Low- z and external constraints on w . In all cases, the existing data are consistent with a cosmological constant ($w = -1$). The DES best-fit χ^2 is 577 with 498 dof. This subset of the final DES data constrains w to within a factor of three of the combined external constraint. This result illustrates the prospects for multiple independent, precise low-redshift constraints on dark energy from upcoming large-scale photometric experiments.

The constraints on all cosmological model parameters are

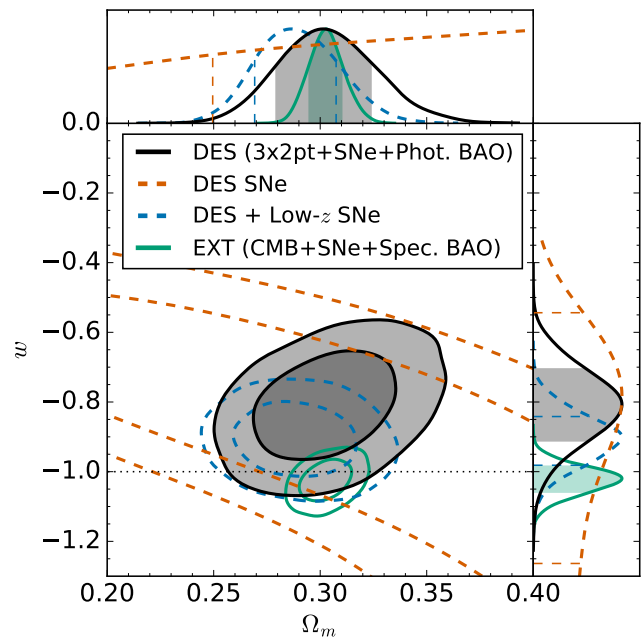


FIG. 2. Constraints on the dark energy equation of state w and Ω_m in a w CDM model with fixed curvature ($\Omega_k = 0$) and marginalized neutrino mass density. We compare constraints from the DES data alone (black contours) to the best available external data (green contours), as in Fig. 1, but also show the impact of including a low-redshift SNe Ia data set (Low- z) to anchor the DES SNe Ia as done in Ref. [19] (blue contours). Each component of the DES analysis was fully blinded.

summarized in Table I. Nuisance parameter constraints are not qualitatively changed from individual probe fits. The DES-only ‘3 \times 2pt’ and SNe data are consistent and individually contribute similar constraining power for w and Ω_Λ . In the Λ CDM model, DES constrains the total matter density to 7% (68% CL), the baryon density to 15%, and the correlation amplitude to 3%, described by $S_8 \equiv \sigma_8 \sqrt{\Omega_m/0.3}$, where σ_8 measures the current-day clustering amplitude. The constraints are comparable in w CDM. Fixing $\Omega_k = 0$, we find the S_8 constraint is improved by a factor of 1.2, but there is otherwise no significant improvement in other parameters. The parameter constraints beyond dark energy are driven by the ‘3 \times 2pt’ measurement. In particular, the baryon density constraint is due to sensitivity to the shape of the matter power spectrum from baryon damping [80]. The constraint on Ω_b from the CMB, by contrast, is also sensitive to the impact of baryons on the acoustic oscillations. Thus future low-redshift survey data will provide another avenue to test the predictions of our models from early Universe observations like the CMB with measurements of Ω_b from surveys like DES.

OUTLOOK

The most precise constraints on dark energy properties require combining cosmological probes that include information from both geometry and growth across cosmic history. Thus far such diverse information was collected from different experiments, which were subject to different calibration and systematic errors. We have combined for the first time in DES the purely cosmographic SN and BAO measurements with the growth-sensitive weak lensing and galaxy clustering measurements to independently place strong constraints on the nature of dark energy. These results share a common set of calibration frameworks and blinding policy across probes. DES has independently constrained Ω_m , Ω_b , Ω_Λ , σ_8 , and w , while marginalizing over a free neutrino mass. We expect future DES results to provide a further factor of 2-4 improvement in these constraints due to increased area, depth, and number of SNe in the final analyses, which will then be followed by subsequent order of magnitude advances from more sensitive photometric surveys of the 2020s.

ACKNOWLEDGEMENTS

Funding for the DES Projects has been provided by the DOE and NSF (USA), MEC/MICINN/MINECO (Spain), STFC (UK), HECCE (UK), NCSA (UIUC), KICP (U. Chicago), CCAPP (Ohio State), MIFPA (Texas A&M), CNPQ, FAPERJ, FINEP (Brazil), DFG (Germany) and the Collaborating Institutions in the Dark Energy Survey.

The Collaborating Institutions are Argonne Lab, UC Santa Cruz, University of Cambridge, CIEMAT-Madrid, University of Chicago, University College London, DES-Brazil Consortium, University of Edinburgh, ETH Zürich, Fermilab, University of Illinois, ICE (IEEC-CSIC), IFAE Barcelona, Lawrence Berkeley Lab, LMU München and the associated Excellence Cluster Universe, University of Michigan, NOAO, University of Nottingham, Ohio State University, University of Pennsylvania, University of Portsmouth, SLAC National Lab, Stanford University, University of Sussex, Texas A&M University, and the OzDES Membership Consortium.

Based in part on observations at Cerro Tololo Inter-American Observatory, National Optical Astronomy Observatory, which is operated by the Association of Universities for Research in Astronomy (AURA) under a cooperative agreement with the National Science Foundation.

The DES Data Management System is supported by the NSF under Grant Numbers AST-1138766 and AST-1536171. The DES participants from Spanish institutions are partially supported by MINECO under grants AYA2015-71825, ESP2015-66861, FPA2015-68048, SEV-2016-0588, SEV-2016-0597, and MDM-2015-0509, some of which include ERDF funds from the European Union. IFAE is partially funded by the CERCA program of the Generalitat de Catalunya. Research leading to these results has received funding from the European Research Council under the

European Union's Seventh Framework Program (FP7/2007-2013) including ERC grant agreements 240672, 291329, and 306478. We acknowledge support from the Australian Research Council Centre of Excellence for All-sky Astrophysics (CAASTRO), through project number CE110001020, and the Brazilian Instituto Nacional de Ciência e Tecnologia (INCT) e-Universo (CNPq grant 465376/2014-2).

This manuscript has been authored by Fermi Research Alliance, LLC under Contract No. DE-AC02-07CH11359 with the U.S. Department of Energy, Office of Science, Office of High Energy Physics. The United States Government retains and the publisher, by accepting the article for publication, acknowledges that the United States Government retains a non-exclusive, paid-up, irrevocable, world-wide license to publish or reproduce the published form of this manuscript, or allow others to do so, for United States Government purposes.

This research used resources of the National Energy Research Scientific Computing Center, a DOE Office of Science User Facility supported by the Office of Science of the U.S. Department of Energy under Contract No. DE-AC02-05CH11231. This work also used resources on the CCAPP condo of the Ruby Cluster at the Ohio Supercomputing Center [81]. Plots in this manuscript were produced partly with MATPLOTLIB [82], and it has been prepared using NASA's Astrophysics Data System Bibliographic Services.

-
- [1] A. G. Riess *et al.* (Supernova Search Team), *Astron. J.* **116**, 1009 (1998).
 - [2] S. Perlmutter *et al.* (Supernova Cosmology Project), *Astrophys. J.* **517**, 565 (1999).
 - [3] A. Albrecht *et al.*, ArXiv e-prints (2006), [arXiv:0609591](https://arxiv.org/abs/0609591).
 - [4] J. Frieman, M. Turner, and D. Huterer, *Ann. Rev. Astron. Astrophys.* **46**, 385 (2008).
 - [5] D. H. Weinberg, M. J. Mortonson, D. J. Eisenstein, C. Hirata, A. G. Riess, and E. Rozo, *Phys. Rep.* **530**, 87 (2013).
 - [6] D. Huterer and D. L. Shafer, *Rept. Prog. Phys.* **81**, 016901 (2018).
 - [7] W. Hu and S. Dodelson, *Ann. Rev. Astron. Astrophys.* **40**, 171 (2002).
 - [8] G. Hinshaw *et al.*, *ApJS* **208**, 19 (2013).
 - [9] Planck Collaboration *et al.*, ArXiv e-prints (2018), [arXiv:1807.06209](https://arxiv.org/abs/1807.06209).
 - [10] D. M. Scolnic *et al.*, *ApJ* **859**, 101 (2018).
 - [11] L. Anderson *et al.*, *MNRAS* **441**, 24 (2014).
 - [12] J. E. Bautista *et al.*, *ApJ* **863**, 110 (2018), [arXiv:1712.08064](https://arxiv.org/abs/1712.08064).
 - [13] S. Alam *et al.*, *MNRAS* **470**, 2617 (2017).
 - [14] S. W. Allen, A. E. Evrard, and A. B. Mantz, *ARA&A* **49**, 409 (2011).
 - [15] S. H. Suyu *et al.*, *MNRAS* **468**, 2590 (2017).
 - [16] R. Mandelbaum, ArXiv e-prints (2017), [arXiv:1710.03235](https://arxiv.org/abs/1710.03235).
 - [17] DES Collaboration *et al.*, *Phys. Rev. D* **98**, 043526 (2018).
 - [18] DES Collaboration *et al.*, ArXiv e-prints (2017), [arXiv:1712.06209](https://arxiv.org/abs/1712.06209).
 - [19] DES Collaboration *et al.*, ArXiv e-prints (2018), [arXiv:1811.02374](https://arxiv.org/abs/1811.02374).
 - [20] R. A. C. Croft and M. Dailey, ArXiv e-prints (2011), [arXiv:1112.3108](https://arxiv.org/abs/1112.3108).

- [21] <http://hsc.mtk.nao.ac.jp/ssp/>.
- [22] <http://kids.strw.leidenuniv.nl>.
- [23] <http://www.darkenergysurvey.org/> ().
- [24] <http://www.lsst.org>.
- [25] <http://sci.esa.int/euclid>.
- [26] <http://wfirst.gsfc.nasa.gov>.
- [27] <http://www.sdss3.org/surveys/boss.php>.
- [28] <https://www.sdss.org/surveys/eboss>.
- [29] <https://www.4most.eu/cms>.
- [30] <https://www.desi.lbl.gov/> ().
- [31] <https://pfs.ipmu.jp>.
- [32] B. Flaugher *et al.* (DES Collaboration), *Astron. J.* **150**, 150 (2015).
- [33] S. Desai *et al.*, *ApJ* **757**, 83 (2012).
- [34] I. Sevilla *et al.* (DES Collaboration), ArXiv e-prints (2011), [arXiv:1109.6741](https://arxiv.org/abs/1109.6741).
- [35] J. J. Mohr *et al.*, in *Observatory Operations: Strategies, Processes, and Systems II*, Proc. SPIE, Vol. 7016 (2008) p. 70160L.
- [36] E. Morganson *et al.* (DES Collaboration), *PASP* **130**, 074501 (2018).
- [37] A. Drlica-Wagner *et al.* (DES Collaboration), *ApJS* **235**, 33 (2018).
- [38] D. A. Goldstein *et al.* (DES Collaboration), *AJ* **150**, 82 (2015).
- [39] R. Kessler *et al.* (DES Collaboration), *AJ* **150**, 172 (2015).
- [40] E. Huff and R. Mandelbaum, ArXiv e-prints (2017), [arXiv:1702.02600](https://arxiv.org/abs/1702.02600).
- [41] E. S. Sheldon and E. M. Huff, *Astrophys. J.* **841**, 24 (2017).
- [42] J. Zuntz *et al.* (DES Collaboration), *MNRAS* **481**, 1149 (2018).
- [43] N. Benítez, *Astrophys. J.* **536**, 571 (2000).
- [44] B. Hoyle *et al.* (DES Collaboration), *MNRAS* **478**, 592 (2018).
- [45] E. Rozo *et al.* (DES Collaboration), *MNRAS* **461**, 1431 (2016).
- [46] J. Elvin-Poole *et al.* (DES Collaboration), *Phys. Rev. D* **98**, 042006 (2018).
- [47] R. Cawthon *et al.* (DES Collaboration), *MNRAS* **481**, 2427 (2018).
- [48] M. Gatti *et al.* (DES Collaboration), *MNRAS* (2018), [10.1093/mnras/sty466](https://arxiv.org/abs/10.1093/mnras/sty466).
- [49] C. Davis *et al.* (DES Collaboration), ArXiv e-prints (2017), [arXiv:1710.02517](https://arxiv.org/abs/1710.02517).
- [50] E. Krause and T. Eifler, *MNRAS* **470**, 2100 (2017).
- [51] E. Krause *et al.* (DES Collaboration), ArXiv e-prints (2017), [arXiv:1706.09359](https://arxiv.org/abs/1706.09359).
- [52] N. MacCrann *et al.* (DES Collaboration), *MNRAS* **480**, 4614 (2018).
- [53] J. Prat *et al.* (DES Collaboration), *Phys. Rev. D* **98**, 042005 (2018).
- [54] M. A. Troxel *et al.* (DES Collaboration), *Phys. Rev. D* **98**, 043528 (2018).
- [55] J. Zuntz *et al.*, *Astronomy and Computing* **12**, 45 (2015).
- [56] C. D’Andrea *et al.* (DES Collaboration), in prep. (2018).
- [57] D. Brout *et al.*, ArXiv e-prints (2018), [arXiv:1811.02378](https://arxiv.org/abs/1811.02378) [astro-ph.IM].
- [58] D. L. Burke *et al.*, *AJ* **155**, 41 (2018).
- [59] J. Lasker *et al.*, ArXiv e-prints (2018), [arXiv:1811.02380](https://arxiv.org/abs/1811.02380).
- [60] R. Kessler *et al.*, ArXiv e-prints (2018), [arXiv:1811.02379](https://arxiv.org/abs/1811.02379).
- [61] R. Kessler and D. Scolnic, *ApJ* **836**, 56 (2017).
- [62] D. Scolnic and R. Kessler, *ApJ* **822**, L35 (2016).
- [63] D. Brout *et al.*, ArXiv e-prints (2018), [arXiv:1811.02377](https://arxiv.org/abs/1811.02377).
- [64] E. Macauley *et al.*, ArXiv e-prints (2018), [arXiv:1811.02376](https://arxiv.org/abs/1811.02376).
- [65] M. Hicken *et al.*, *ApJ* **700**, 1097 (2009).
- [66] M. Hicken *et al.*, *ApJS* **200**, 12 (2012).
- [67] C. Contreras *et al.*, *AJ* **139**, 519 (2010).
- [68] M. Crocce *et al.* (DES Collaboration), *MNRAS*, 2411 (2018).
- [69] S. Avila *et al.* (DES Collaboration), *MNRAS* **479**, 94 (2018).
- [70] A. J. Ross *et al.* (DES Collaboration), *MNRAS* **472**, 4456 (2017).
- [71] K. C. Chan *et al.* (DES Collaboration), *MNRAS* **480**, 3031 (2018).
- [72] H. Camacho *et al.* (DES Collaboration), ArXiv e-prints (2018), [arXiv:1807.10163](https://arxiv.org/abs/1807.10163).
- [73] Planck Collaboration, P. A. R. Ade, *et al.*, *A&A* **594**, A13 (2016).
- [74] Planck Collaboration, P. A. R. Ade, *et al.*, *A&A* **594**, A15 (2016).
- [75] Planck Collaboration, N. Aghanim, *et al.*, *A&A* **594**, A11 (2016).
- [76] D. Scolnic *et al.*, *ApJ* **815**, 117 (2015).
- [77] F. Beutler *et al.*, *Mon. Not. Roy. Astron. Soc.* **416**, 3017 (2011).
- [78] A. J. Ross *et al.*, *Mon. Not. Roy. Astron. Soc.* **449**, 835 (2015).
- [79] For further discussion of the χ^2 value, see [83] (Sec. 4 on Light Curve fitting and bias corrections).
- [80] This constraint on Ω_b is not prior driven, despite being degenerate with A_s and n_s (which is unconstrained).
- [81] OSC, “Ohio supercomputer center,” <http://osc.edu/ark:/19495/f5s1ph73> (1987).
- [82] J. D. Hunter, *Computing In Science & Engineering* **9**, 90 (2007).
- [83] <https://des.ncsa.illinois.edu/releases/sn>.